II International Conference on Particle-based Methods - Fundamentals and Applications
PARTICLES 2011
E. Oñate and D.R.J. Owen (Eds)

KELVIN-HELMHOLTZ INSTABILITY BY SPH

M. S. Shadloo*, M. Yildiz†

Faculty of Engineering and Natural Sciences, Advanced Composites & Polymer Processing Laboratory, Sabanci University, 34956 Tuzla, Istanbul, Turkey.
*e-mail: mostafa@sabanciuniv.edu, www.msshadloo.com
†e-mail: meyildiz@sabanciuniv.edu

Key words: Smoothed Particle Hydrodynamics (SPH), Shear flow, Two-Phase flow, Interfacial flows, Surface tension, Kelvin-Helmholtz Instability (KHI).

Abstract. In this paper, we have modeled the *Kelvin-Helmholtz Instability* (KHI) problem of an incompressible two-phase immiscible fluid in a stratified inviscid shear flow with interfacial tension using *Smoothed Particle Hydrodynamics* (SPH) method. The time dependent evolution of the two-fluid interface over a wide range of Richardson number (Ri) and for three different density ratios is numerically investigated. The simulation results are compared with analytical solutions in the linear regime. It was observed that the SPH method requires a Richardson number lower than unity (*i.e.*, $Ri \cong 0.8$) for the onset of KHI, and that the artificial viscosity plays a significant role in obtaining physically correct simulation results that are in agreement with analytical solutions. The numerical algorithm presented in this work can easily handle a two-phase fluid flow with various density ratios.

1 INTRODUCTION

Flow instability at the interface between two horizontal parallel streams of different velocities and densities, with the heavier fluid at the bottom, is called the Kelvin-Helmholtz Instability (KHI). The KHI is induced by either velocity shear within a continuous fluid or a sufficiently large velocity difference across the interface of a multiphase fluid. The instability kicks in when the destabilizing effect of shear across the interface overcomes the stabilizing effect of stratification due to gravity and/or surface tension if it exists. The KHI manifests itself as a row of horizontal eddies (in the form of waves) aligned across the interface. These eddies or waves are referred to as main billows. There are several well-known natural situations where the KHI can be observed such as wind blowing over the ocean or water surface, a meteor entering the Earth's atmosphere, the interface between the tails of comets and solar wind, or the interface between a liquid layer and a compressible gas, among others.

The Kelvin-Helmholtz instability problem was solved first for the ideal case of inviscid and incompressible fluids in 1871 by Lord Kelvin. It has been studied both theoretically [1] and experimentally [2], as well as numerically [3, 4].

Smoothed Particles Hydrodynamics (SPH) is one of the most successful Lagrangian methods which was introduced separately by Gingold and Monaghan and Lucy in 1977 initially to simulate astrophysical problems. Due to its flexibility and capability of modeling complex engineering problems, the SPH method has been extensively used for solving a wide variety of problems [5, 6]. As well, there are some recently reported works which have been conducted to investigate the feasibility and the ability of the SPH method to capture the physics behind the KHI [7, 8].

The aim of this work is to simulate the KHI by using a Weakly Compressible SPH (WCSPH) method, thereby showing the ability of the SPH technique to capture this hydrodynamic instability for various density ratios. The current presentation differs from earlier works in the following aspects: the previously reported relevant works treated the fluid to be compressible whereas here it is treated as an incompressible liquid. Unlike other pertinent SPH papers, this paper systematically examines the effects of the stabilizing parameters (e.g. surface tension (σ) and stratifying body force ($\Delta\rho\mathbf{g}$)) individually or concurrently on the occurrence of the KHI for a wide range of Ri numbers and three density ratios.

2 SMOOTHED PARTICLE HYDRODYNAMICS

SPH is a Lagrangian particle-based method which has been extensively used over a decade for solving partial differential equations (thermo mechanical balance laws integrated with relevant constitutive equations) for both fluids and solids dynamic problems.In comparison to mesh-dependent approaches, the SPH method significantly facilitates the handling of the problems with free or interfacial surface, whose locations are priori unknown and have to be computed during the solution of the problem since the position of particles determine the final configuration of the flow domain. Therefore, it is a particularly powerful tool to study multiphase fluid flow problems.

The term *particles* merely refers to movable points that represent fluid elements in three dimensional space, and each particle is associated with mass, density, velocity and other relevant hydrodynamics properties. In another way of saying, the continuum under the consideration is discretized into finite number of field points which are known as particles. Field variables carried by each particle are calculated through an interpolation (weighting, smoothing, kernel) function, $W(r_{\mathbf{ij}}, h)$ from those of surrounding neighbor particles. Here, $r_{\mathbf{ij}}$ is the magnitude of the distance vector ($\vec{\mathbf{r}}_{\mathbf{ij}} = \vec{\mathbf{r}}_{\mathbf{i}}\text{-}\vec{\mathbf{r}}_{\mathbf{j}}$) between the particle of interest $\mathbf{i}$ (an interpolated particle) and its neighboring particles $\mathbf{j}$ (neighbors of the interpolated particle), and h is called smoothing length, which is an important input parameter that controls the number of active neighbor particles within the support domain of smoothing function. Here, $\vec{\mathbf{r}}_{\mathbf{i}}$ and $\vec{\mathbf{r}}_{\mathbf{j}}$ are the position vectors for particles $\mathbf{i}$ and $\mathbf{j}$, respectively. The weighting function should have the following attributes; the normalization, the Dirac-delta

function, the compactness, and spherically symmetric even function properties. Due to the compactness property, $W(r_{\mathbf{ij}}, h) = 0$ when $r_{\mathbf{ij}} > h$, in computations, a given particle interacts with only its nearest neighbors contained within the radius of support domain h.

For an arbitrary function (scalar (A), vectorial ($\vec{\mathbf{A}}$), or tensorial ($\underline{\underline{\mathbf{A}}}$), the kernel approximation in the form of the integral representation can be written as

$$A(\vec{\mathbf{r}}_\mathbf{i}) \cong \langle A(\vec{\mathbf{r}}_\mathbf{i}) \rangle \equiv \int_{Space} A(\vec{\mathbf{r}}_\mathbf{j}) W(r_{\mathbf{ij}}, h) d^3\vec{\mathbf{r}}_\mathbf{j}. \tag{1}$$

where the angle bracket $\langle\rangle$ denotes the kernel approximation.

In the SPH method, it is common practice to replace the integral operation with a summation over all the particles within the support domain of the kernel function (*i.e.* $r_{\mathbf{ij}} < h$). In what follows, one can write

$$A_\mathbf{i} = A(\vec{\mathbf{r}}_\mathbf{i}) = \frac{1}{\psi_\mathbf{i}} \sum_\mathbf{j} A_\mathbf{j} W_\mathbf{ij} \tag{2}$$

where we have used a concise notation (*i.e.* $W(r_{\mathbf{ij}}, h) = W_\mathbf{ij}$), and the differential volume element $d^3\vec{\mathbf{r}}_\mathbf{j}$ is approximated by the reciprocal of the number density $\psi_\mathbf{i}$, which is defined for the particle $\mathbf{i}$ as

$$\psi_\mathbf{i} = \sum_\mathbf{j} W_\mathbf{ij}, \tag{3}$$

By using a differentiable kernel, the spatial derivative of the function A evaluated at the location of particle $\mathbf{i}$ can be simply reduced to an ordinary differentiation of the interpolant function $W_\mathbf{ij}$ with respect to the particle $\mathbf{i}$ times the volume and the field variables of neighbor particles. It is due to this analytical approximation that the SPH method does not require a grid. For example, one of the widely used SPH gradient discretization scheme of the field A can be written in the form of

$$\nabla_\mathbf{i} A_\mathbf{i} = \nabla_{\vec{\mathbf{r}}_\mathbf{i}} A(\vec{\mathbf{r}}_\mathbf{i}) = \frac{1}{\psi_\mathbf{i}} \sum_\mathbf{j} (A_\mathbf{j} - A_\mathbf{i}) \nabla_\mathbf{i} W_\mathbf{ij}. \tag{4}$$

where $\nabla_{\vec{\mathbf{r}}_\mathbf{i}} A(\vec{\mathbf{r}}_\mathbf{i})$ or in a concise notation $\nabla_\mathbf{i} A_\mathbf{i}$ denotes the spatial derivative of the field A with respect to $\mathbf{i}^{th}$ particle coordinates. Since the kernel function determines the extent of the interaction between the particle of interest and its neighbors, its choice is related to the accuracy, efficiency, and stability of the resulting algorithm. In this work, the quintic kernel based on the fifth-order spline function is adopted [9].

2.1 Governing Equations

The governing equations used to solve the fluid problems in this article are the mass and linear momentum balance equations which are expressed in the Lagrangian form and given in the direct notation as

$$\frac{d\rho}{dt} = -\rho\nabla\cdot\vec{\mathbf{v}}, \tag{5}$$

$$\rho\frac{d\vec{\mathbf{v}}}{dt} = -\nabla p + \rho\vec{\mathbf{g}} + \vec{\mathbf{F}}^{\sigma}, \tag{6}$$

where p is the pressure, $\vec{\mathbf{v}}$ is the fluid velocity, and $\vec{\mathbf{F}}^{\sigma}$ denotes a force per unit volume exerted on the fluid-fluid interface due to surface tension. Here, it should be pointed out that in reality, the surface tension force on the fluid-fluid interface is a surface force (*i.e.*, force per unit area). For the sake of computational efficiency and simplifications, we here have followed a common practice whereby the surface tension force per unit area is included in the momentum balance equation as the force per unit volume. As written in eq.(12),this volume force is proportional to product of the interface gradient (gradient of the color field used to distinguish two fluids) and the surface curvature. This approach is referred to as the continuum surface force (CSF) formulation and is widely used in modeling surface tension force of multiphase fluid flows. Also, it should be noted that due to the inviscid fluid assumption, the linear momentum balance equation does not have a viscous force term.

In the WCSPH method, for enforcing the incompressibility condition, the density can be evolved either using eq. (5) in combination with eq. (4) or directly utilizing the number density approach as given in eq. (7).

$$\rho_{\mathbf{i}} = m_{\mathbf{i}}\psi_{\mathbf{i}} \tag{7}$$

As for the balance of linear momentum equation, the acceleration term can be discretized in the general form of

$$\vec{\mathbf{a}}_{\mathbf{i}} = \frac{1}{m_{\mathbf{i}}}\vec{\mathbf{F}}_{\mathbf{i}}, \tag{8}$$

where $\vec{\mathbf{F}}_{\mathbf{i}}$ is the total force acting on the particle $\mathbf{i}$, which can be written in the discrete form as

$$\vec{\mathbf{F}}_{\mathbf{i}} = m_{\mathbf{i}}\vec{\mathbf{g}} + \vec{\mathbf{F}}_{\mathbf{i}}^{\sigma} - \sum_{\mathbf{j}}\left[(\frac{p_{\mathbf{i}}}{\psi_{\mathbf{i}}^2} + \frac{p_{\mathbf{j}}}{\psi_{\mathbf{j}}^2}) + \Pi_{\mathbf{ij}}\right]\nabla_{\mathbf{i}}W_{\mathbf{ij}}. \tag{9}$$

Here, the first term in the summation sign ($p_{\mathbf{i}}/\psi_{\mathbf{i}}^2 + p_{\mathbf{j}}/\psi_{\mathbf{j}}^2$) is the discretized form of the pressure gradient force and $\Pi_{\mathbf{ij}}$ is artificial viscosity.

The artificial viscosity term is included in the current model in order for circumventing numerical instabilities due to the meshless nature of the SPH method. This term introduces some numerical diffusion into the model, thus preventing non-physical oscillations. There are various forms of artificial viscosity terms in SPH literature. In this work, we have implemented the one suggested by Monaghan in [10] in the form of

$$\Pi_{\mathbf{ij}} = -\frac{8\mu_{\mathbf{ij}}(\vec{\mathbf{v}}_{\mathbf{ij}} \cdot \vec{\mathbf{r}}_{\mathbf{ij}})}{\psi_{\mathbf{i}}\psi_{\mathbf{j}}(r_{\mathbf{ij}}^2 + \epsilon h_m^2)} \tag{10}$$

where $\vec{\mathbf{v}}_{\mathbf{ij}} = \vec{\mathbf{v}}_{\mathbf{i}} - \vec{\mathbf{v}}_{\mathbf{j}}$, $\vec{\mathbf{r}}_{\mathbf{ij}} = \vec{\mathbf{r}}_{\mathbf{i}} - \vec{\mathbf{r}}_{\mathbf{j}}$, $h_m = \frac{h_{\mathbf{i}}+h_{\mathbf{j}}}{2}$, $\epsilon \approx 0.0001$ is introduced to prevent singularity when $r_{\mathbf{ij}} = 0$ and $\mu_{\mathbf{ij}}$ is harmonic average of $\mu_{\mathbf{i}}$ and $\mu_{\mathbf{j}}$ defined by

$$\mu_{\mathbf{ij}} = \frac{2}{\frac{1}{\mu_{\mathbf{i}}} + \frac{1}{\mu_{\mathbf{j}}}}, \tag{11}$$

where $\mu_{\mathbf{i}} = \frac{1}{8}\alpha h_{\mathbf{i}} c_{\mathbf{i}} \rho_{\mathbf{i}}$ in which c is sound speed and α is the artificial viscosity constant.

In accordance with the continuum surface force (CSF) formulation, the surface tension force term in eq.(9) is formulated as

$$\vec{\mathbf{F}}_{\mathbf{i}}^{\sigma} = \sigma_{\mathbf{i}}\kappa_{\mathbf{i}}\vec{\mathbf{n}}_{\mathbf{i}}\delta_s, \tag{12}$$

where $\kappa_{\mathbf{i}}$ is the interface curvature, and $\vec{\mathbf{n}}_{\mathbf{i}}$ is the unit vector normal to interface and δ_s is the interface dirac delta function($\delta_s = |\nabla C|$).

The unit vector normal to the fluid-fluid interface $\vec{\mathbf{n}}_{\mathbf{i}}$ is

$$\vec{\mathbf{n}}_{\mathbf{i}} = \frac{\nabla_{\mathbf{i}} C_{\mathbf{i}}}{|\nabla_{\mathbf{i}} C_{\mathbf{i}}|}. \tag{13}$$

where $\nabla_{\mathbf{i}} C_{\mathbf{i}}$ is computed as.

$$\nabla_{\mathbf{i}} C_{\mathbf{i}} = \sum_{\mathbf{j}} \frac{C_{\mathbf{ji}}}{\bar{\psi}_{\mathbf{ij}}} \nabla_{\mathbf{i}} W_{\mathbf{ij}}. \tag{14}$$

where $\bar{\psi}_{\mathbf{ij}} = (\psi_{\mathbf{i}} + \psi_{\mathbf{j}})/2$ and $C_{\mathbf{ji}} = C_{\mathbf{j}} - C_{\mathbf{i}}$.

Finally, the interface curvature $\kappa_{\mathbf{i}}$ is calculated from

$$\kappa_{\mathbf{i}} = \sum_{\mathbf{j}} \frac{1}{\bar{\psi}_{\mathbf{ij}}} \vec{\mathbf{n}}_{\mathbf{ij}} \cdot \nabla_{\mathbf{i}} W_{\mathbf{ij}}, \tag{15}$$

where $\vec{\mathbf{n}}_{\mathbf{ij}} = \vec{\mathbf{n}}_{\mathbf{i}} - \vec{\mathbf{n}}_{\mathbf{j}}$.

2.2 Time Integration

In order to increment the time-steps in the SPH algorithm, we have used a Velocity Verlet predictor corrector method [10]. This technique is an explicit time integration scheme, and is relatively simple to implement. The time integration scheme starts with the predictor step to compute the intermediate particle positions based on current particles' velocities as follow

$$\vec{\mathbf{r}}_{\mathbf{i}}^{n+\frac{1}{2}} = \vec{\mathbf{r}}_{\mathbf{i}}^{n} + \frac{\Delta t}{2}\vec{\mathbf{v}}_{\mathbf{i}}^{n}. \tag{16}$$

where n is the temporal index.

Afterward, new densities for each particles are calculated from eq.(3) and eq.(7) at current intermediate particle positions. Since fluid is assumed weakly compressible, the artificial equation of state of the form

$$p - p_o = c^2(\rho - \rho_o), \tag{17}$$

is used to compute new pressure values at current particle positions. This state equation enforces the incompressibility condition on the flow such that a small variation in density produces a relatively large change in pressure hence preventing the dilatation of the fluid. Here, c is artificial sound velocity and the subscript o denotes the reference condition. The speed of sound for each particle must be chosen carefully to ensure that the fluid is very closely incompressible. In this work, upon selecting the sound speed twenty times larger than the maximum fluid velocity, the density variation is limited to one percent. Having computed the acceleration of each particle from eq.(8) using the current pressure and velocity values, one can obtain the velocity of new time-step through the time integration as

$$\vec{\mathbf{v}}_{\mathbf{i}}^{n+1} = \vec{\mathbf{v}}_{\mathbf{i}}^{n} + \vec{\mathbf{a}}_{\mathbf{i}}^{n+\frac{1}{2}}\Delta t. \tag{18}$$

Finally, the position of each particle is corrected at the new time-step based on this velocity. It is to be noted that in the SPH method, the order of particles affects the accuracy of interpolations for gradient and Laplacian computations. Therefore, for the computational stability and accuracy, it is preferable to move the SPH particles in a more orderly fashion, which can be achieved through using the XSPH technique proposed by Monaghan et.al [10]. The XSPH method includes the contribution from neighboring particles, thereby causing a fluid particle to move with an average velocity

$$\vec{\mathbf{r}}_{\mathbf{i}}^{n+1} = \vec{\mathbf{r}}_{\mathbf{i}}^{n+\frac{1}{2}} + \frac{\Delta t}{2}\vec{\mathbf{v}}_{\mathbf{i}}^{*n+1}, \tag{19}$$

where $\vec{\mathbf{v}}_{i}^{*n+1}$ is the XSPH-averaged new velocity by the correction factor of 0.1.

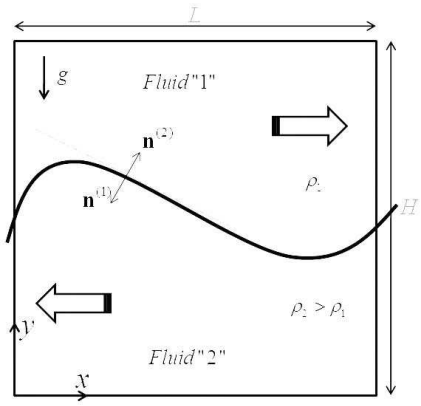

Figure 1: Configuration of the Kelvin-Helmholtz instability at the initial time step.

3 Definition of The Problem

The KHI can occur at the interface between two horizontal parallel streams of different velocities and densities, with the heavier fluid at the bottom. For the simulation of this natural flow phenomenon, we here consider two immiscible fluids that are intervened between two infinite parallel horizontal plate with the height of H ($0 < y < H$) (Fig.1). For simplicity, the x-dimension of the computational domain L ($0 < x < L$) is chosen to be equal to the domain height H ($L = H$).

The computational domain for the KHI problem is represented by a set of particles created on a Cartesian grid with an equidistant particle spacing. At the beginning of the simulations, the computational domain is halved by a horizontal midline ($H_1 = H_2 = \frac{H}{2}$ and $H = 1m$), where each half represents a different fluid region. The number of particles for each fluid region is the same. An initial sinusoidal perturbation is applied to the fluid-fluid interface through switching the type of particles near the midline. The wavelength of the initial disturbance is set to be equal to the domain length ($\lambda = L$) so that the instability is to be confined into mid section of the model domain. The magnitude of the perturbation is $\zeta_o/H \approx 0.03$ where ζ_o is the initial amplitude of the applied disturbance. Let U_1 and ρ_1 be the velocity and density of the basic state of the upper layer and U_2 and ρ_2 be those of the bottom layer. Particles of two fluids initially at rest are set into motion in opposite directions with the same magnitude ($i.e.$ $U_1 = -U_2 = U = 0.5\frac{m}{s}$).

To be able to show the effect of density on the KH instability, in simulations we have used several density ratios $\frac{\rho_2}{\rho_1} = 2$, 5 and 10 where ρ_1 is set to be $\rho_1 = 1000\frac{kg}{m^3}$. When all modeling parameters are active, the surface tension force acts (σ) only on the interface particles in the direction of the unit normal whereas gravity (g) acts in the downward direction on all particles. For determining the number of SPH particles for the particle number independent results, we run several test cases where three different particle arrays, namely, 80×80, 150×150 and 300×300 were used. It was observed that the 150×150 array of particles is sufficient for capturing primary wave as well as obtaining particle-

independent solutions.

4 RESULTS

For unstable situations, the analytical non-dimensional growth rate G_e in the linear regime can be written as [11]

$$G_e = Im(\omega) = \frac{2\pi\sqrt{\rho_1\rho_2}}{\rho_1+\rho_2}\sqrt{1-Ri}. \tag{20}$$

where Ri is the dimensionless Richardson number

$$Ri = \frac{\rho_1+\rho_2}{k\rho_1\rho_2(U_1-U_2)^2}\left(g(\rho_2-\rho_1)+k^2\sigma\right). \tag{21}$$

For numerical investigation, the numerical growth rate G_n is calculated in the form of

$$G_n = \frac{\hat{\zeta}/\zeta_o - 1}{t^*}, \tag{22}$$

where $\hat{\zeta}$ is the amplitude of the disturbance at time t and t^* is the dimensionless time.

$$t^* = \frac{t\,|U_2-U_1|}{H}, \tag{23}$$

where t is real time and H is domain height.

To be able to compare the analytical growth rate in eq.(20) with the numerical one in eq.(22), (because eq.(20) is only valid for the linear regime), $\hat{\zeta}$ and t^* are calculated when the wave amplitude reaches to 10 percentage of the domain height ($\hat{\zeta} \cong 0.1H$).

Having perturbed the fluid-fluid interface at the initial time ($t^* = 0$) by a small disturbance, under certain input parameters (*i.e.*, surface tension, gravity, density, *etc.*), the interface disturbance grows and the flow system becomes unstable. Fig.2 illustrates the growth of the interface disturbance as a function of time in the two-dimensional KHI problem for the density ratios of $\frac{\rho_2}{\rho_1} = 2$ and $\frac{\rho_2}{\rho_1} = 10$ at $Ri = 0.01$. For this simulation, the artificial viscosity coefficient in eq.(10) is set to be $\alpha = 0.001$. As a result of the interface disturbance, the heavier fluid starts moving in a positive vertical direction, while the lighter fluid in the opposite direction. Thus, both fluids begin to penetrate into each other. As the time progresses, the height of the instability gets larger, and due to the inertial effect, both fluids tend to gain horizontal velocity opposite to their initial bulk velocities. A small vortex appears and the flow regime is no longer linear. This process results in the formation of the main billow. It should be noted that the linear stability growth rate formula is valid only before this time step. At later times, the characteristic form of the KHI becomes much more obvious. Passing time, the non-linear flow regime results in the formation of a Cat's Eye vortex and the fingering phenomenon for the density ratios of $\frac{\rho_2}{\rho_1} = 2$ and $\frac{\rho_2}{\rho_1} = 10$, respectively.

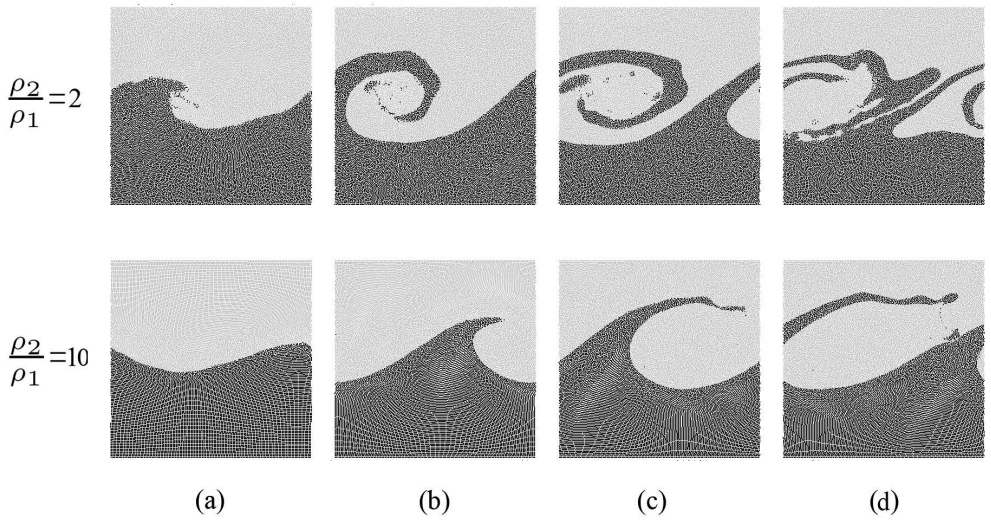

(I)

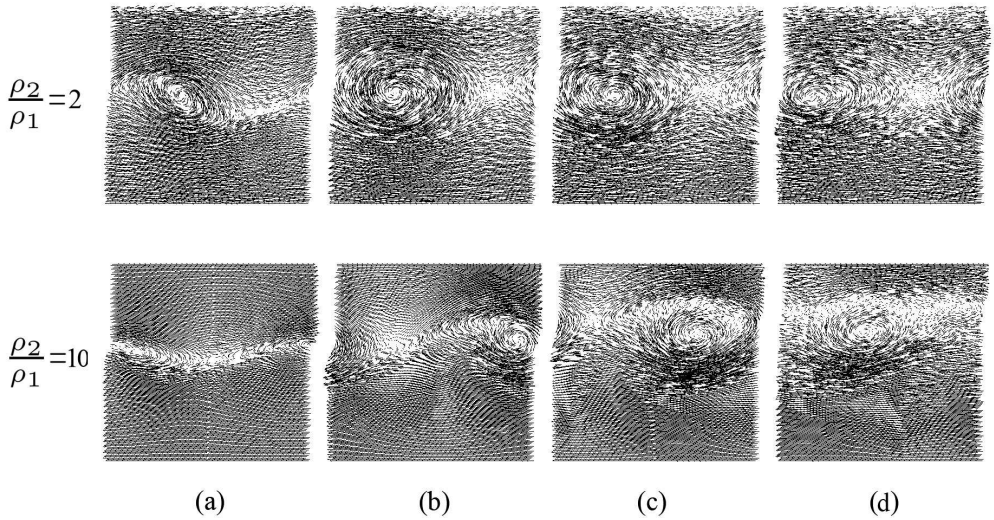

(II)

Figure 2: Time evolution of the interface in the two-dimensional KHI problem with the density ratios of $\frac{\rho_2}{\rho_1} = 2$ and $\frac{\rho_2}{\rho_1} = 10$, and the $Ri = 0.01$; (a)$t^* = 1.0$, (b)$t^* = 2.0$, (c)$t^* = 3.0$, (d)$t^* = 4.0$; (I) particle distributions and (II) velocity vectors.

In the simulation with the density ratio of 2, both fluids have relatively close inertial forces, and therefore, the vortex is not advected significantly by fluid streams. Consequently, as the simulation progresses, the flow circulation forms the Cat's Eye shape. On the other hand, due to the fact that there exists a relatively large difference in the inertial forces between the upper and the lower fluid layers for the density ratio of 10 , and the heavier fluid at the bottom of the modeling domain has a greater inertial force than the lighter fluid at the top, the flow circulation is advected faster in the flow direction of the heavier fluid whereby it leaves the flow domain through the left side and re-enters it from the right side. Accordingly, the translational motion of the flow circulation along the interface brings about the elongation of the crest of the wave, or the fingering phenomenon.

From eq.(20) it is also notable that for a given density ratio, the Ri number is the only parameter that controls the stability of the two fluid system in the KHI phenomena. Towards this end, it is important to determine the critical value for this number, which defines the border between stable and unstable flow regimes. The results of the simulations have shown that in the SPH method, the critical value for the Ri number is approximately 0.8 for all density ratios, which is slightly smaller than the one determined using the linear stability analysis. This difference might be attributed to the artificial viscosity utilized in the SPH method, numerical diffusion and the methodology used to perturb the initial fluid-fluid interface.

Fig. 3a shows a plot of the growth rate versus the Ri number in which numerically and analytically computed growth rates are compared. One can see from the figure that the numerically computed growth rate decreases with increasing Ri number and/or density ratio, which is consistent with eq.(20), and simulation results are in close agreement with those corresponding to analytical solutions. The comparison of results presented in figs.2 and 3 for the density ratios of 2 and 10 for a given Ri number reveals that the density ratio significantly affects the shape of the main billow as well as the growth rate. It is also important to note that with increasing density ratio, the transition from a linear to non-linear regime is delayed to later simulation times.

The artificial viscosity is one of the reasons that may cause numerically obtained simulation results to deviate slightly from analytical ones. Fig. 3b illustrates the effect of the artificial viscosity on the time evolution of the interface in the two-dimensional KHI problem for one specific test case, which is chosen as a representative for the whole data. In this specific test case, $\frac{\rho_2}{\rho_1} = 10$. As seen from the figure, upon choosing a low artificial viscosity coefficient, the numerical results are in better agreement with those of the linear stability analysis. One can also notice that the growth rate decreases as the utilized artificial viscosity coefficient increases. To have stable numerical simulations, the artificial viscosity coefficient can not be chosen to be too small (as an example, $\alpha \geq 0.0001$ and 0.001 for $\frac{\rho_2}{\rho_1} = 2$ and for $\frac{\rho_2}{\rho_1} = 10$, respectively). Therefore, it should be selected carefully in order to have physically valid numerical results, which can predict the KHI phenomena accurately without loosing numerical stability.

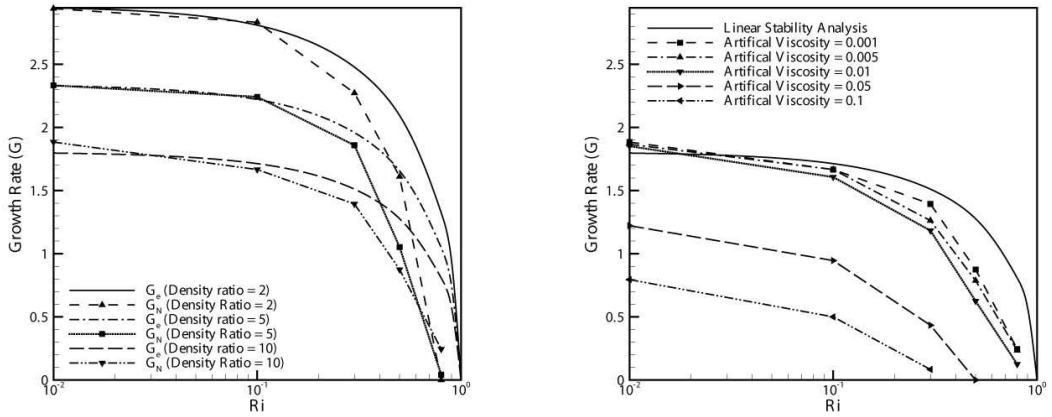

(a) (b)

Figure 3: Growth rates G of KHI in the linear regime for various Richardson numbers and (a) the effect of density ratios ($\alpha = 0.001$) and (b) the effect of artificial viscosities ($\frac{\rho_2}{\rho_1} = 10$).

5 CONCLUSIONS

The SPH method has been used to simulate Kelvin-Helmholtz instabilities in two-dimensional incompressible two-phase flows under the inviscid assumption through taking the effect of surface tension and body forces into account. Simulations were performed for numerous Richardson numbers, density ratios and artificial viscosities. It was shown that under the influence of certain input parameters (body force, surface tension, and density ratios), a flow instability develops in a two-phase fluid system with an initially disturbed fluid-fluid interface. This instability grows in time and, subsequently, the flow system experiences a transition from a linear to a non-linear regime. It was also illustrated that all simulations results are in reasonably good agreement in terms of growth rate with those corresponding to analytical solutions of the linear stability analysis for KHI. The noted discrepancies between numerical analytical results might be attributed to numerical diffusions, to the inclusion of artificial viscosity and to the nature of the initial disturbance of the fluid-fluid interface. Additionally, it was observed that the growth rate is higher for lower density ratio and Richardson numbers, and reaches to free shear flow limit at Richardson numbers near zero. Based on the linear stability analysis, for Richardson numbers lower than unity ($Ri < 1$), the flow can be unstable, but for the numerical method used in this paper, the flow instability occurs at (Ri) number values less than roughly 0.8. Numerical results suggest that for a given density ratio, the growth rate of the instability is only controlled by the Richardson number, and independent of the nature of stabilizing forces. Also it is shown that the artificial viscosity plays a significant role in all simulation, therefore, it should be chosen such that it preserves the stability of the numerical method as well as captures all complex physics behind this phenomenon.

ACKNOWLEDGMENT

Funding provided by the European Commission Research Directorate General under Marie Curie International Reintegration Grant program with the Grant Agreement number of 231048 (PIRG03-GA-2008-231048) is gratefully acknowledged. The first author also acknowledges the Yousef Jameel Scholarship.

REFERENCES

[1] Lamb H. *Hydrodynamics*. Dover Publications, 1932.

[2] Lin PY, Hanrattty TJ. Prediction of the initiation of slugs with linear stability theory. *International journal of multiphase flow* 1986; **12**(1):79–98.

[3] Zhang R, He X, Doolen G, Chen S. Surface tension effects on two-dimensional two-phase Kelvin–Helmholtz instabilities. *Advances in Water Resources* 2001; **24**(3-4):461–478.

[4] Herrmann M. A Eulerian level set/vortex sheet method for two-phase interface dynamics. *Journal of Computational Physics* 2005; **203**(2):539–571.

[5] Monaghan JJ. Simulating free surface flows with sph. *Journal of Computational Physics* 1994; **110**:399–406.

[6] Shadloo MS, Zainali A, Sadek SH, Yildiz M. Improved incompressible smoothed particle hydrodynamics method for simulating flow around bluff bodies. *Computer Methods in Applied Mechanics and Engineering* 2011; **200**(9-12):1008 – 1020.

[7] Agertz O, Moore B, Stadel J, Potter D, Miniati F, Read J, Mayer L, Gawryszczak A, Kravtsov A, Nordlund A, *et al.*. Fundamental differences between SPH and grid methods. *Monthly Notices of the Royal Astronomical Society* 2007; **380**(3):963–978.

[8] Price DJ. Modelling discontinuities and Kelvin-Helmholtz instabilities in SPH. *Arxiv preprint arXiv:0709.2772* 2007; .

[9] Morris JP. *Analysis of Smoothed Particle Hydrodynamics with Applications*. Monash University, 1996.

[10] Monaghan JJ. Smoothed particle hydrodynamics. *Reports on Progress in Physics* 2005; **68**:1703–1759.

[11] Shadloo MS, Yildiz M. Numerical modeling of kelvinhelmholtz instability using smoothed particle hydrodynamics. *International Journal for Numerical Methods in Engineering* 2011; doi:10.1002/nme.3149.